Article

In Situ Generation of Carboxylate: An Efficient Strategy for a One-Pot Synthesis of Homo- and Heterometallic Polynuclear Complexes

Konstantin S. Gavrilenko, Sergey V. Punin, Olivier Cador,
Stphane Golhen, Lahcne Ouahab, and Vitaly V. Pavlishchuk

J. Am. Chem. Soc., **2005**, 127 (35), 12246-12253• DOI: 10.1021/ja050451p • Publication Date (Web): 13 August 2005

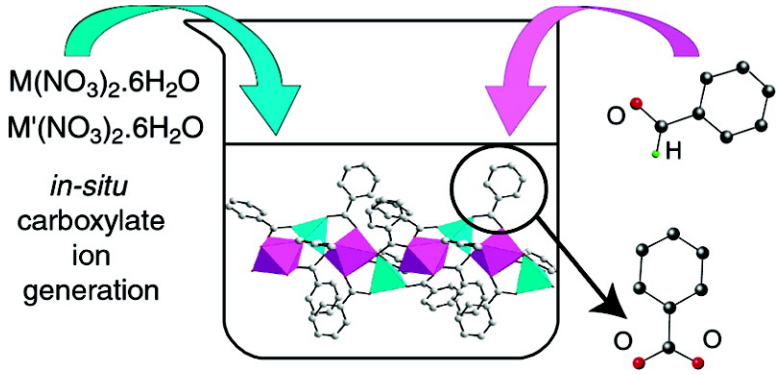

More About This Article

Additional resources and features associated with this article are available within the HTML version:

- Supporting Information
- Links to the 6 articles that cite this article, as of the time of this article download
- Access to high resolution figures
- Links to articles and content related to this article
- Copyright permission to reproduce figures and/or text from this article

View the Full Text HTML

J|A|C|S
ARTICLES
Published on Web 08/13/2005

In Situ Generation of Carboxylate: An Efficient Strategy for a One-Pot Synthesis of Homo- and Heterometallic Polynuclear Complexes

Konstantin S. Gavrilenko,[†,‡] Sergey V. Punin,[‡] Olivier Cador,[†] Stéphane Golhen,[†] Lahcène Ouahab,*[,†] and Vitaly V. Pavlishchuk*[,‡]

Contribution from the Laboratoire de Chimie du Solide et Inorganique Moléculaire, UMR 6511 CNRS-Université de Rennes 1, Institut de Chimie de Rennes, Avenue du Général Leclerc, 35042 Rennes Cedex, France, and L. V. Pisarzhevskii Institute of Physical Chemistry of the National Academy of Sciences of the Ukraine, prospekt Nauki 31, 03028 Kiev, Ukraine

Received January 23, 2005; E-mail: lahcene.ouahab@univ-rennes1.fr; shchuk@inphyschem-nas.kiev.ua

Abstract: An efficient strategy for synthesis of a wide range of homo- and heterometallic polynuclear complexes is proposed. The synthesis protocol consists of a two-step one-pot reaction. The first step is the in situ generation of carboxylate anions via oxidation of aromatic aldehydes by metal nitrates in air. The aldehydes act as solvents and are also involved in redox processes. Solutions containing solely transition metal cations and aromatic carboxylates are obtained following this procedure. The second step is a tunable "*à la carte*" formation of a series of various polynuclear carboxylato complexes from solutions obtained at the former stage upon addition of different solvents. The polarity and donor properties of the solvents play a key role in determination of the nuclearities of the complexes. Hydrolytic processes can induce the formation of oxo- or hydroxo-bridges inside the polynuclear core as well. Complexes of various nuclearities are obtained: from discrete tri-, hexa-, or octanuclear units to 1D polymers. This protocol can be adapted with disconcerting simplicity to the synthesis of heterometallic species with similar molecular structures to their homometallic analogues starting from stoichiometric mixture of metal nitrates under the same reaction conditions. Detailed description of synthesis and the molecular structure of one representative complex for each series are presented in this paper. The temperature dependence of magnetic susceptibility of the heterometallic 1-D MnCo chain reveals typical behavior of a ferrimagnetic chain. The low-temperature investigations on single crystals show significant Ising type magnetic anisotropy.

Introduction

Transition metal polynuclear carboxylate complexes are currently widely investigated, especially, for the following important reasons: (i) besides 1D, 2D, or 3D magnetic ordering which takes place in carboxylate containing compounds,[1] it has been found that even individual molecules of such complexes could behave as individual magnets at low temperature, the so-called *Single-Molecule Magnets* (SMM);[2] (ii) theses complexes are also successfully used as biomimetic models of some polymetallic active centers of enzymes;[3] (iii) these polynuclear complexes can be viewed as extended models of intermediates during the geosediments formation;[4] (iv) these compounds can efficiently catalyze different unique organic reactions due to the ability of polymetallic centers to coordinate and to activate several functional groups of a substrate;[5] (v) recently, it has been demonstrated that some polynuclear carboxylate complexes can be used as precursors for synthesis of nanosized magnetic oxides.[6] Hence, the development of a new strategy for synthesis of polynuclear skeletons which can lead to a wide variety of

[†] Université de Rennes 1.

[‡] Pisarzhevskii Institute of Physical Chemistry of the National Academy of Sciences of the Ukraine.

(1) (a) Ruiz-Pérez, C.; Rodríguez-Martín, Y.; Hernández-Molina, M.; Delgado, F. S.; Pasán, J.; Sanchiz, J.; Lloret, F.; Julve, M. *Polyhedron* **2003**, *22*, 2111. (b) Midollini, S.; Orlandini, A.; Rosa, P.; Sorace, L. *Inorg. Chem.* **2005**, *44*, 2060. (c) Mao, J.-G.; Clearfield, A. *Inorg. Chem.* **2002**, *41*, 2319. (d) Gil de Muro, I.; Mautner, F. A.; Insausti, M.; Lezama, L.; Arriortua, M. I.; Rojo. T. *Inorg. Chem.* **1998**, *37*, 3243. (e) Ang, S. G.; Sun, B. W.; Gao, S. *Inorg. Chem. Commun.* **2004**, *7*, 795. (f) Zhang, X.; Huang, D.; Chen, F.; Chen, C.; Liu Q. *Inorg. Chem. Commun.* **2004**, *7*, 662. (g) Wang, X.-Y.; Wei, H.-Y.; Wang, Z.-M.; Chen, Z.-D.; Gao, S. *Inorg. Chem.* **2005**, *44*, 572. (h) Manson, J. L.; Lancaster, T.; Chapon, L. C.; Blundell, S. J.; Schlueter, J. A.; Brooks, M. L.; Pratt, F. L.; Nygren, C. L.; Qualls, J. S. *Inorg. Chem.* **2005**, *44*, 989.

(2) (a) Gatteschi, D.; Sessoli, R. *Angew. Chem., Int. Ed.* **2003**, *42*, 2 and references therein. (b) Rumberger, E. M.; Zakharov, L. N.; Rheingold, A. L.; Hendrickson, D. N. *Inorg. Chem.* **2004**, *43*, 6531. (c) Brechin, E. K.; Sanudo, E. C.; Wernsdorfer, W.; Boskovic, C.; Yoo, J.; Hendrickson, D. N.; Yamaguchi, A.; Ishimoto, H.; Concolino, T. E.; Rheingold, A. L.; Christou, G. *Inorg. Chem.* **2005**, *44*, 502. (d) King, P.; Wernsdorfer, W.; Abboud, K. A.; Christou, G. *Inorg. Chem.* **2004**, *43*, 7315. (e) Oshio, H.; Nihei, M.; Yoshida, A.; Nojiri, H.; Nakano, M.; Yamaguchi, A.; Karaki, Y.; Ishimoto, H. *Chem.—Eur. J.* **2005**, *11*, 843. (f) Sanudo, E. C.; Wernsdorfer, W.; Abboud, K. A.; Christou, G. *Inorg. Chem.* **2004**, *43*, 4137.

(3) Wu, A. J.; Penner-Hahn, J. E.; Pecoraro, V. L. *Chem. Rev.* **2004**, *104*, 903 and references therein. Ferreira, K. N.; Iverson, T. M.; Maghlaoui, K.; Barber, J.; Iwata, S. *Science* **2004**, *303*, 1831.

(4) Pierre, T. G. St.; Chan, P.; Bauchspiess, K. R.; Webb, J.; Betteridge, S.; Walton, S.; Dickson D. P. E. *Coord. Chem. Rev.* **1996**, *151*, 125.

(5) (a) Tapper, A. E.; Long, J. R.; Staples, R. J.; Stavropoulos, P. *Angew. Chem., Int. Ed.* **2000**, *39*, 2343. (b) Marr, S. B.; Carvel, R. O.; Richens, D. T.; Lee, H.-J.; Lane, M.; Stavropoulos, P. *Inorg. Chem.* **2000**, *39*, 4630.

(6) Gavrilenko, K. S.; Mypnyuk, T. V.; Il'in, V. G.; Orlyk, S. M.; Pavlishchuk, V. V. *Theor. Exp. Chem. (Rus. Ed.)* **2002**, *38*, 110.

 10.1021/ja050451p CCC: $30.25

unknown topologies of polynuclear framework is still an actual challenge in modern coordination chemistry.

So far, various methods have been developed to synthesize polynuclear complexes. Actually, in most cases, researchers are guided by intuitive approaches. In overwhelming cases polynuclear carboxylate cores are synthesized employing nucleophilic substitution reactions[7] such as hydrolytic processes where polynuclear complexes are formed by the oligomerization of the oxo- or hydroxo building blocks. A similar reaction mechanism is employed in most polynuclear core reactions with polydentate amphyphilic agents (polyamines, amino alcohols, etc.).[2b,c,7] In some cases, redox reactions are employed to change the oxidation states of metal ions.[2d,e,8] Metal salts in high oxidation state (MnO_4^-, $Cr_2O_7^{2-}$, etc.) are reduced in the presence of appropriate ligands by organic compounds or metal ions. Some of metal ions, such as Mn(II), Co(II), Fe(II), can be easily oxidized to their higher oxidation states in the presence of appropriate ligands by atmospheric oxygen or hydrogen peroxide. In all the above-mentioned cases, the carboxylate ligand was already incorporated in coordination core or was involved in the reaction solely as nucleophile and not participate in any redox process during the reaction. Furthermore, metal carboxylate salts are not soluble in noncoordinating solvents, and this leads to the limitation of their use as starting materials. Scarce information about polynuclear complex formation accompanied by ligand redox processes are available so far.[2f,9] However, as a rule such reactions are by-processes which accompany the main reaction of polynuclear core formation. Up to now redox transformation of ligands during the formation of polynuclear framework complexes was not considered as a possible route to achieve different types of polynuclear topologies. However such processes are promising for the building of new types of homo- and heterometallic polynuclear complexes because redox intermediates can change the reaction route.

We propose in this paper a new efficient procedure for synthesis of polynuclear species based on in-situ redox generation of carboxylate ligands leading to both homo- and heterometallic discrete tri-, hexa-, and octanuclear complexes, as well as to 1D-coordination polymers. The detailed synthetic procedure and X-ray structures for one compound from each series are given. The magnetic properties of the new heterometallic MnCo chain are presented.

Experimental Section

Synthesis. Chemicals were used as purchased without further purification.

$[Co(PhCOO)_2]_n$ (Ia): $Co(NO_3)_2 \cdot 6H_2O$ (582 mg, 2 mmol) was heated with benzaldehyde (5 mL) during 10 min. The resulting blue solution was cooled and toluene (5 mL) was added. After several hours crystals were collected by filtration, washed with toluene and dried in a vacuum. Yield is 566 mg (94%, based on Co). Anal. Calcd for $CoC_{14}H_{10}O_4$: C, 55.8; H, 3.35; Co, 19.6. Found: C, 56.0; H, 3.42; Co, 19.5%.

$[Co(PhCOO)_2]_n$ (Ib): $Co(NO_3)_2 \cdot 6H_2O$ (582 mg, 2 mmol) was heated with benzaldehyde (5 mL) during 10 min, toluene was then added to the boiling blue solution. After cooling, the resulting violet crystals were filtered off, washed with toluene, and dried in a vacuum. Yield 554 mg (92%, based on Co). Anal. Calcd for $CoC_{14}H_{10}O_4$: C, 55.8; H, 3.35; Co, 19.6. Found: C, 56.1; H, 3.39; Co, 19.7%.

$[Co_3(PhCOO)_6(py)_2]$ (II): A mixture of $Co(NO_3)_2 \cdot 6H_2O$ (582 mg, 2 mmol) and benzaldehyde (5 mL) was heated to boiling during 10 min. Then pyridine (0.2 mL, ~2 mmol) was added, and the resulting reaction mixture was heated further for 5 min. After cooling to 80 °C, 0.2 mL of acetonitrile was added. Next day, deposited red crystals were filtered off, washed with acetonitrile followed by a small amount of pyridine, and air-dried. Yield is 0.502 g (71%). Anal. Calcd for $Co_3C_{52}H_{40}N_2O_{12}$: C, 58.8; H, 3.80; N, 2.64; Co, 16.7. Found: C, 58.9; H, 3.95; Co, 16.7%.

$[Co_6(OH)_2(PhCOO)_{10}(PhCOOH)_4]\cdot 3PhCH_3$ (III·3PhCH$_3$): A mixture of $Co(NO_3)_2 \cdot 6H_2O$ (400 mg, 1.37 mmol) and benzaldehyde (10 mL) was heated to boiling during 10 min. Then the reaction mixture was cooled, and toluene (10 mL) was added. Water (2 mL) was layered, and the reaction mixture was left undisturbed. After 1 month, red-violet crystals were filtered off, washed with toluene, and air-dried. Yield is 0.152 g (28%). Anal. Calcd for $Co_6C_{119}H_{99}O_{30}$: C, 60.5; H, 4.22; Co, 15.0. Found: C, 60.3; H, 4.15; Co, 15.2%.

$[Co_8O_4(PhCOO)_{12}(CH_3CN)_3(H_2O)]\cdot 2CH_3CN$ (IV·2CH$_3$CN): A mixture of $Co(NO_3)_2 \cdot 6H_2O$ (582 mg, 2 mmol) and benzaldehyde (10 mL) was heated to boiling for 10 min. Then reaction mixture was cooled, acetonitrile (10 mL) was added, and the reaction mixture was left undisturbed on air for 1 h. Acetonitrile was evaporated under vacuum, and ether (10 mL) was added. Hexane (20 mL) was added to the green solution, and dark oil was separated. It was extracted by 30 mL of a boiling acetonitrile/ether (1:5) mixture and slowly evaporated in air. Within 1 day, dark green crystals were collected by filtration, washed with acetonitrile, and air-dried. Yield is 0.275 g (49%, based on Co). Anal. Calcd for $Co_8C_{94}H_{77}N_5O_{29}$: C, 51.0; H, 3.51; N, 3.17; Co, 21.3. Found: C, 50.8; H, 3.49; N, 3.13; Co, 21.2%.

$[Ni_2Mn(PhCOO)_6(py)_4]\cdot 2CH_3CN$ (V·2CH$_3$CN): It was prepared similarly to **II** using a mixture of $Ni(NO_3)_2 \cdot 6H_2O$ (582 mg, 2 mmol) and $Mn(NO_3)_2 \cdot 6H_2O$ (287 mg, 1 mmol). Yield is 0.597 g (46%, based on Mn). Anal. Calcd for $Ni_2MnC_{66}N_6H_{56}O_{12}$: C, 60.1; H, 4.35; N, 6.48; Ni, 9.0; Mn, 4.2. Found: C, 59.9; H, 4.26; N, 6.34; Ni, 9.1; Mn, 4.3%.

$[Co_2Ni_4(OH)_2(PhCOO)_{10}(PhCOOH)_4]$ (VI): It was prepared similarly to **III·3PhCH$_3$** using a mixture of $Ni(NO_3)_2 \cdot 6H_2O$ (1.16 g, 4 mmol) and $Co(NO_3)_2 \cdot 6H_2O$ (582 mg, 2 mmol). Yield is 0.668 g (16%, based on Co). Anal. Calcd for $Ni_4Co_2C_{98}H_{76}O_{30}$: C, 56.4; H, 3.67; Ni, 11.3; Co, 5.6. Found: C, 56.6; H, 3.72; Ni, 11.2; Co, 5.7%.

$[CoMn(PhCOO)_4]_n$ (VII): A mixture of $Co(NO_3)_2 \cdot 6H_2O$ (582 mg, 2 mmol) and $Mn(NO_3)_2 \cdot 6H_2O$ (574 mg, 2 mmol) was heated with benzaldehyde (5 mL) until a precipitate appears. The solution was cooled to room temperature, and toluene (5 mL) was added. After 1 h, violet crystals were filtered off, washed with toluene and ether, and air-dried. Yield 1080 mg (90%, based on Co). Anal. Calcd for $CoMnC_{28}H_{20}O_8$: C, 56.2; H, 3.37; Co, 9.8; Mn, 9.2. Found: C, 56.3; H, 3.41; Co, 9.7; Mn, 9.0%.

$[Co(p\text{-}MePhCOO)_2]_n$ (VIII): $Co(NO_3)_2 \cdot 6H_2O$ (582 mg, 2 mmol) was heated with *p*-methylbenzaldehyde (5 mL) until the beginning of crystallization. The reaction mixture was cooled, and toluene (5 mL) was added. Violet crystals were filtered off, washed with toluene thoroughly, and dried in a vacuum. Yield is 608 mg (92%, based on Co). Anal. Calcd for $CoC_{16}H_{14}O_4$: C, 58.4; H, 4.29; Co, 17.9. Found: C, 58.5; H, 4.34; Co, 17.8%.

Crystallographic Data Collection and Structure Determination. Single crystals were mounted on a Nonius four circle diffractometer equipped with a CCD camera and a graphite monochromated Mo K_α

(7) (a) Adams, H.; Fenton, D. E.; McHugh, P. E. *Inorg. Chem. Commun.* **2004**, *7*, 140. (b) Tsohos, A.; Dionyssopoulou, S.; Raptopoulou, C. P.; Terzis, A.; Bakalbassis, E. G.; Perlepes, S. P. *Angew. Chem., Int. Ed.* **1999**, *38*, 983. (c) Gavrilenko, K. S.; Vertes, A.; Vanko, G.; Kiss, L. F.; Addison, A. W.; Weyhermüller, T.; Pavlishchuk, V. V. *Eur. J. Inorg. Chem.* **2002**, 3347. (d) Canada-Vilalta, C.; O'Brien, T. A.; Brechin, E. K.; Pink, M.; Davidson, E. R.; Christou, G. *Inorg. Chem.* **2004**, *43*, 5505.
(8) (a) Abbati, G. L.; Cornia, A.; Fabretti, A. C.; Caneschi, A.; Gatteschi, D. *Inorg. Chem.* **1998**, *37*, 3759−3766. (b) Thompson, L. K.; Kelly, T. L.; Dawe, L. N.; Grove, H.; Lemaire, M. T.; Howard, J. A. K.; Spencer, E. C.; Matthews, C. J.; Onions, S. T.; Coles, S. J.; Horton, P. N.; Hursthouse, M. B.; Light, M. E. *Inorg. Chem.* **2004**, *43*, 7605. (c) Dimitrou, K.; Brown, A. D.; Concolino, T. E.; Rheingold, A. L.; Christou, G. *Chem. Commun.* **2001**, 1284.
(9) Kim, J.; Cho, H. *Inorg. Chem. Commun.* **2004**, *7*, 122.

Table 1. Crystal Data and Structure Refinement Parameters for **I**, **II**, **III·3PhCH$_3$**, **V·2CH$_3$CN**, **VI**, and **VII** Compounds

	I	II	III·3PhCH$_3$	V·2CH$_3$CN	VI	VII
empirical formula	$CoC_{14}H_{10}O_4$	$Co_3C_{52}H_{40}N_2O_{12}$	$Co_6C_{119}H_{99}O_{30}$	$MnNi_2C_{66}H_{56}N_6O_{12}$	$Co_2Ni_4C_{98}H_{76}O_{30}$	$CoMnC_{28}H_{20}O_8$
fw	301.15	1061.65	2362.56	1297.53	2086.29	598.31
T, K	293(2)	293(2)	293(2)	110(2)	293(2)	293(2)
crystal system	orthorhombic	triclinic	monoclinic	triclinic	monoclinic	orthorhombic
space group	*Pcab*	$P\bar{1}$	*P*21/*n*	$P\bar{1}$	*P*21/*c*	*Pcab*
a, Å	10.5031(1)	10.4764(2)	17.4460(3)	11.3534(1)	18.7936(3)	10.6761(2)
b, Å	18.9228(3)	10.5116(2)	20.5552(5)	11.9927(2)	20.8663(4)	19.1023(5)
c, Å	25.0747(5)	10.9597(2)	20.2288(6)	23.2928(4)	25.3089(6)	24.996(1)
α, (deg)	90	85.320(1)	90	98.732(1)	90	90
β, (deg)	90	86.288(1)	101.267(1)	90.811(1)	106.229(1)	90
γ, (deg)	90	88.897(1)	90	106.525(1)	90	90
V, Å^3	4983.6(1)	1200.26(4)	5543.3(2)	2999.75(8)	9529.5(3)	5097.7(3)
Z	16	1	2	2	4	8
d_{calc}, g cm^{-3}	1.606	1.469	1.415	1.437	1.454	1.559
unique reflns	6899	10 969	9994	13 627	1682	4647
R(int)	0.0366	0.0274	0.0372	0.0446	0.0483	0.0479
GOF on F^2	1.034	1.008	1.044	0.865	1.007	1.032
R_1[a] [$I > 2\sigma(I)$]	0.0491	0.0502	0.0474	0.0531	0.0590	0.0441
wR_2[b]	0.1126	0.1321	0.1162	0.1455	0.1417	0.1033

[a] $R_1 = \Sigma||F_o| - |F_c||/\Sigma|F_o|$. [b] $wR_2 = \{\Sigma[w(F_o^2 - F_c^2)^2]/\Sigma[w(F_o^2)^2]\}^{1/2}$.

radiation source ($\lambda = 0.710\ 73$ Å), from the Centre de Diffractométrie (CDFIX), Université de Rennes 1, France. Data for **V·2CH$_3$CN** were collected at 110 K to prevent any acetonitrile solvent lost, and all other data were collected at 293 K. Effective absorption correction was performed (SCALEPACK[10]). Structures were solved with a direct method using the SHELXS-97 program and refined with a full matrix least-squares method on F^2 using the SHELXL-97 program. Crystallographic data are summarized in Table 1. Complete crystal structure results as a CIF file including bond lengths, bond angles, and atomic coordinates are deposited as Supporting Information.

Magnetic Measurements. The magnetizations have been recorded with a Quantum Design MPMS SQUID magnetometer operating in the temperature range 2−300 K with a DC magnetic field up to 5 T. The experimental data have been corrected from the diamagnetism of the sample holder, and the intrinsic diamagnetism of the materials were evaluated with Pascal's tables.

Results and Discussion

Synthesis. It is known that the formation of polynuclear complexes is strongly dependent on numerous factors including synthetic conditions and reagents ratio. For example, oxidation of Mn(II) acetate by permanganate results in the formation of different types of tri-, tetra-, or dodecanuclear complexes, depending on the reaction conditions, i.e., solvent, reaction temperature, Mn(VII)/Mn(II) ratio, and the presence of additional components, such as pyridine or other amines.[8]

Generation of carboxylates from appropriate precursors in the reaction mixture is the key point of the proposed strategy. It worth noticing that pure metal benzoate salts cannot not be used as starting materials because they are not soluble in noncoordinating solvents. Aromatic aldehydes and transition metal nitrates have been used as starting reagents. Due to the absence of α-hydrogen atoms as well as the exceptional stability of aromatic rings, only carboxylate species are formed as oxidation products. Moreover, the utilization of nitrate anion as oxidizer avoids the presence in the resulting reaction mixture of additional species which may act as potential participants in a further process of polynuclear skeleton construction. Thus the first step consists of the in situ redox generation of carboxylate ligands by oxidation of aromatic aldehydes by metal nitrates under aerobic conditions. The reaction of nitrate with aldehyde is accompanied by vigorous release of water vapor and NO_2. This reaction can be described by the following equation:

$$2PhCHO + 3NO_3^- = 2PhCOO^- + 3NO_2\uparrow + H_2O\uparrow + e^-$$

It is evident from this equation that an additional oxidizer is required to complete aldehyde oxidation. Therefore the reaction can be performed under aerobic conditions, and finally the equation becomes:

$$4PhCHO + 4NO_3^- + O_2 = 4PhCOO^- + 4NO_2\uparrow + 2H_2O\uparrow$$

Accordingly the resulting solution contains only transition metal cations and carboxylate anions. Hereafter, we will refer to it as "metal carboxylate solution".

The final stage consists of an *"à la carte"* synthesis of various polynuclear complexes by adjusting the appropriate conditions in the same pot. Crystallizations of different polynuclear complexes from the reaction mixture are determined by their solubility and the crystal lattice energy. The added solvent during the second step plays an important role in isolation of polynuclear compounds; it may be involved as a solvate adduct in crystal lattice or as a ligand coordinated to the metallic core. The introduction of additional ligands such as heterocyclic amines into the reaction mixture at the second stage is also important for formation of μ_n-oxo- or μ_n-hydroxo-bridges in the metallic core. We illustrate this strategy using cobalt nitrate and benzaldehyde as starting materials. Different types of homometallic polynuclear complexes are thus obtained (Scheme 1, route **A**). Heating $Co(NO_3)_2 \cdot 6H_2O$ with benzaldehyde yields a violet blue "cobalt benzoate solution". In nonpolar medium (toluene) 1D-polymer $[Co(PhCOO)_2]_n$ **I** crystallizes as two phases: monoclinic **Ia**, the structure of which was published before,[11] and orthorhombic **Ib**. The monoclinic phase is obtained by adding toluene to cold "cobalt benzoate solution", while the addition of toluene to hot solution yields the orthorhombic phase.

The proposed method allows us to reduce the time scale of synthesis of complex **Ia** from days[11] to hours. The addition of

(10) Otwinowski, Z.; Minor, W. Processing of X-ray Diffraction Data Collected in Oscillation Mode. In *Methods in Enzymology, Volume 276: Macromolecular Crystallography, Part A*; Carter, C. W., Jr., Sweet, R. M., Eds.; Academic Press: 1997; pp 307−326.

(11) Spohn, M.; Strähle, J. *Z. Naturforsch.* **1988**, *43B*, 540.

Scheme 1. Routes to Various Homo- and Heteropolynuclear Complexes; Py = Pyridine; A and B Routes Deal with Homometallic and Heterometallic Compounds, Respectively

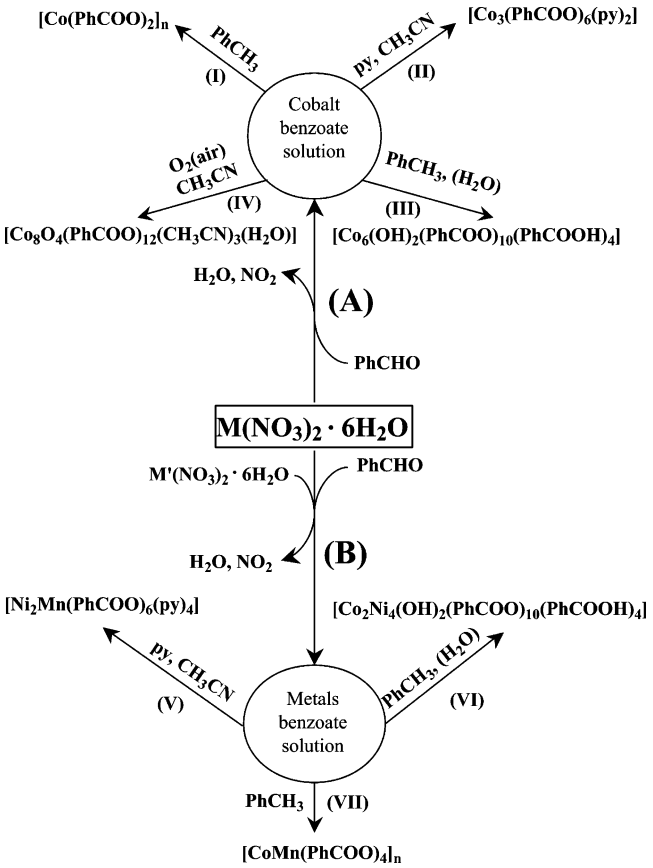

pyridine to cobalt−benzoate solution results in formation of linear trinuclear complex $[Co_3(PhCOO)_6(py)_2]$ **II**. No influence was found of the Co/py ratio on the length of the oligomeric fragment: the formation of the trinuclear moiety was always observed. Complexes with similar metallic core structures were previously reported with different peripheral ligands.[12] Partial hydrolysis of "cobalt benzoate solution" by addition of toluene saturated with water results in crystallization of the hexanuclear complex $[Co_6(OH)_2(PhCOO)_{10}(PhCOOH)_4]$ **III**. Finally, aerobic oxidation in the presence of acetonitrile leads to the octanuclear complex $[Co_8O_4(PhCOO)_{12}(CH_3CN)_3(H_2O)]$ **IV**.[13] Thus depending on the conditions of the second stage it is possible to isolate discrete polynuclear complexes and coordination polymers from "cobalt benzoate solution". The addition of solvents with lower polarity yields complexes with higher nuclearity up to polymeric compounds. This approach was extended successfully to other aromatic aldehydes such as *p*-methylbenzaldehyde which leads to formation of $[Co(p\text{-}MePhCOO)_2]_n$ complex **VIII**.

Remarkably, the proposed method enables the isolation of corresponding heterometallic complexes, using appropriate stoichiometric ratio of metals at the first stage. Heating the stoichiometric 1:1 molar ratio of $Co(NO_3)_2{\cdot}6H_2O$ and $Mn(NO_3)_2{\cdot}6H_2O$ in benzaldehyde leads to "metals benzoate solution" (Scheme 1, route **B**). The addition of toluene to this solution results in formation of violet chain $[CoMn(PhCOO)_4]_n$ **VII**. Starting from manganese and nickel nitrates (1:2) at the first stage followed by pyridine addition yields the heterometallic trinuclear complex $[Ni_2Mn(PhCOO)_6(py)_4]$ **V**. Finally hexanuclear heterometallic compound $[Co_{2Ni4}(OH)_2(PhCOO)_{10}(PhCOOH)_4]$ **VI** is formed starting from the stoichiometric mixture of cobalt and nickel nitrates (1:2).

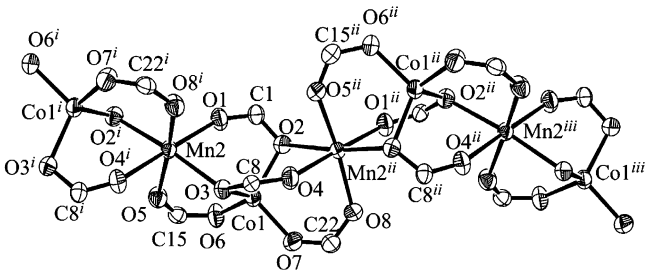

Figure 1. Labeled ORTEP plot at the 50% ellipsoid probability level of the 1-D polymeric chain of **VII** along the *a* axis; aromatic rings are omitted for clarity ((i) $x - {}^1/_2, {}^1/_2 - y, z$; (*ii*) ${}^1/_2 + x, {}^1/_2 - y, z$; (iii) $1 + x, y, z$).

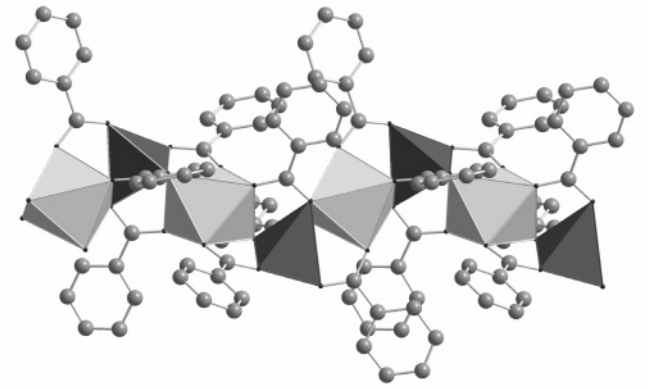

Figure 2. 1-D Polymeric chain of $[CoMn(PhCOO)_4]_n$ with alternating $[MnO_6]$ octahedra and $[CoO_4]$ tetrahedra.

Crystal Structure Analysis. $[Co(PhCOO)_2]_n$ (Ib), $[CoMn(PhCOO)_4]_n$ (VII). These two compounds are isostructural, and therefore, we present here structural details for **VII** and give the corresponding data for **Ib** in brackets. The crystal structure of **VII** (Figure 1) consists of infinite zigzag chains developing along the *a* axis. Two carboxylate anions possess $\mu_2(\eta_1,\eta_1)$ coordination mode while the two others are in $\mu_3(\eta_1,\eta_2)$ mode. The metal ions are alternatively located in tetrahedral $[CoO_4]$ and octahedral $[MnO_6]$ coordination polyhedra and form zigzag chains (Figure 2). The Co−Mn−Co angle is equal to 171.13(2)° [171.45(1)°], and Mn...Co distances are 3.2338(7) and 3.2664(7) Å [3.1657(4) and 3.1957(4) Å]. These quasi-linear trimetallic units are connected thanks to the Co ion, and the angle between two trimetallic units is 110.8° [111.6°]. Cobalt and manganese are connected by oxygen atoms from benzoate anions. In the chain O5, O6 and O7, O8 act as η_1 ligands of $\mu_2(\eta_1,\eta_1)$ bridges. O3 and O2 are η_2 ligands whereas O1, O4 are η_1 ligands. Both O1, O2 and O3, O4 belong to $\mu_3(\eta_1,\eta_2)$ bridging ligands. No significant short contacts are observed between chains.

$[Co_3(PhCOO)_6(py)_2]$ (II). The structure is shown in Figure 3. It consists of a centrosymmetric trimetallic unit: one central cobalt ion (Co1) lying on an inversion center in an octahedral coordination sphere made up of six oxygens from six benzoate

(12) (a) Ye, B.-H.; Chen, X.-M.; Xue, F.; Ji, L.-N.; Mak, T. C. W. *Inorg. Chim. Acta* **2000**, *299*, 1. (b) Reynolds, R. A., III; Dunham, W. R.; Coucouvanis, D. *Inorg. Chem.* **1998**, *37*, 1232. (c) Clegg, W.; Little, I. R.; Straughan, B. P. *Inorg. Chem.* **1988**, *27*, 1916. (d) Catterick, J.; Hursthouse, M. B.; New, D. B.; Thornton, P. *J. Chem. Soc. Chem. Commun.* **1974**, 843.

(13) Dimitrou, K.; Sun, J.-S.; Folting, K.; Christou, G. *Inorg. Chem.* **1995**, *34*, 4160.

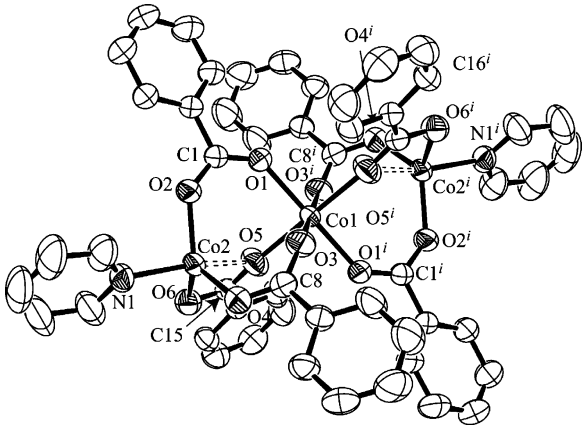

Figure 3. Labeled ORTEP plot at the 50% ellipsoid probability level of the molecule **II** ((i) $-x, -y, -z$). The hydrogen atoms are omitted for clarity.

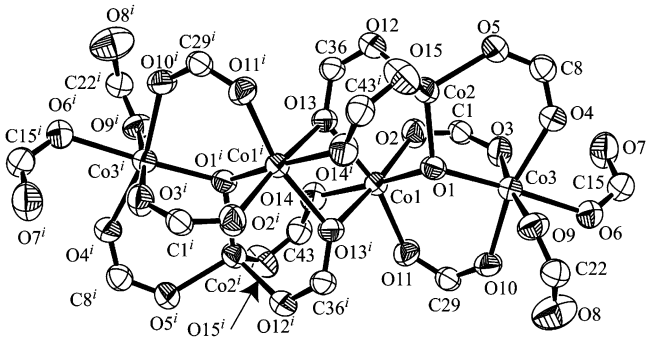

Figure 4. Labeled ORTEP plot at the 50% ellipsoid probability level of the molecule **III**; aromatic rings and hydrogen atoms were omitted for clarity ((i) $1 - x, -y, -z$).

ions acting as an η_1 ligand and two peripheric cobalt ions (Co2) in a distorted bipyramidal surrounding; the Co1...Co2 distance is equal to 3.5455(2) Å. Two benzoate anions are $\mu_2(\eta_1,\eta_1)$ (O1, O2 and O3, O4) bridging ligands and the remaining one $\mu_2(\eta_1,\eta_2)$ ligand (O5, O6). The octahedral coordination sphere of Co1 is quite regular as cobalt−oxygen distances are ranging from 2.069(2) to 2.099(2) Å and the corresponding angles range from 87.54(6)° to 92.46(6)°. These bond lengths are slightly lower than those in similar acetate[12a,b] and crotonate[12c] carboxylate complexes of Co(II) and quite similar to those found in trinuclear benzoate $[Co_3(PhCOO)_6(quin)_2]$.[12d] The Co2 ion is bounded to four oxygen atoms and one nitrogen atom: Three oxygens from three different benzoate anions with Co2...O bonds ranging from 1.951(1) Å to 2.012(2) Å, one nitrogen from a pyridine ring Co2−N1 = 2.062(2) Å, the fifth position is occupied by the O5 atom from a $\mu_2(\eta_1,\eta_2)$ benzoate ligand with Co2...O5 = 2.382(2) Å. Similar coordination arrangement around the Co ion was found in similar cobalt carboxylate complexes.[12]

$[Co_6(OH)_2(PhCOO)_{10}(PhCOOH)_4]\cdot 3PhCH_3$ (III·3PhCH$_3$). The structure consists of a centrosymmetric hexametallic unit, made of four cobalt ions in a distorted octahedral oxygen coordination sphere (Co1 and Co3) and two cobalt ions (Co2) in a tetrahedral oxygen coordination sphere; the coordination sphere is made of oxygen atoms arising from ten benzoate anions, four molecules of benzoic acid, and two OH^- groups (see Figure 4). One toluene molecule lies in a special position, and one in a general position. In the asymmetric unit Co1, Co2, and Co3 are connected via μ_3 OH^- ion (O1). The $[Co1O_6]$ octahedron presents rhombic deformation: three Co−O bonds are longer than 2.1 Å; the longest Co1−O13 bond is equal to 2.210(2) Å; the remaining Co−O distances are ranging from 2.023(2) Å (for Co1−O11) to 2.093(2) Å (for Co1−O14). The $[Co3O_6]$ octahedron is less distorted: the longest distance is Co3−O9 = 2.160(2) Å whereas the shortest is Co3−O1 = 2.045(2) Å. The $[Co2O_4]$ is quite regular with Co2−O bond distances ranging from 1.942(3) to 1.976(2) Å. In the asymmetric unit, only one benzoate group is $\mu_3(\eta_1$-O12, η_2-O13) ligand due to space group symmetries; O13 atom and its crystallographic equivalent yield one shared octahedron edge. The remaining benzoates are $\mu_2(\eta_1,\eta_1)$ bridges. Two η_1-O6 and η_1-O9 from two benzoic acid molecules complete the octahedral oxygen coordination sphere. All metals are bounded to the same OH^- group: Co1 is bounded to three η_1 and two η_2 oxygens from five benzoate anions whereas Co3 is bounded to five η_1 oxygens (O3, O4, O6, O9, O10) from three benzoate anions and two benzoic acid molecules. The tetrahedral Co2 is also bounded to three η_1 oxygen atoms (O5, O12, O15). The Co...Co shortest distance led to two quasi equilateral Co triangles with Co...Co distances ranging from 3.360(1) to 3.410(1) Å, the distance between two Co ions from different triangles is Co1−Co1 = 3.295(1) Å (see Figure 5). No short intermolecular contacts are observed.

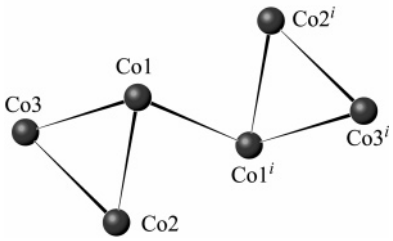

Figure 5. Metal triangles in **III** with interatomic distances: Co1...Co2 = 3.3605(6) Å; Co1...Co3 = 3.4101(7) Å; Co2...Co3 = 3.3935(6) Å; Co1...Co1^i = 3.2947(9) Å; (i) $1 - x, -y, -z$.

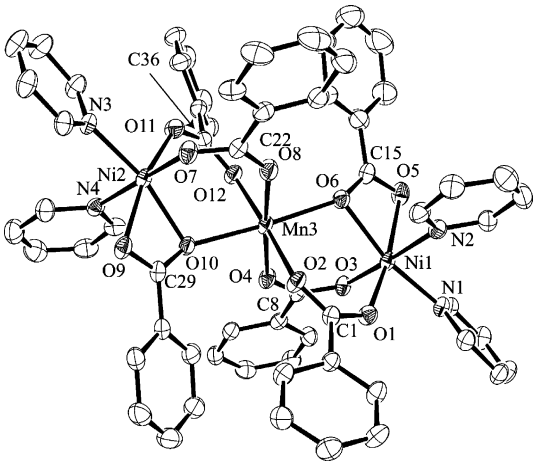

Figure 6. Labeled ORTEP plot at the 50% ellipsoid probability level of the molecule **V** at 110 K. Hydrogen atoms are omitted for clarity.

$[Ni_2Mn(PhCOO)_6(py)_4]\cdot 2CH_3CN$ (V·2CH$_3$CN). The molecule is located in a general position but it is quasi centrosymmetric (see Figure 6). It consists of a central manganese ion (Mn3) in an octahedral coordination sphere of six oxygen atoms from six benzoate ions. Four of them act as η_1 ligands in the equatorial plane (O4, O8, O2, O12) with Mn3−O bond distances ranging from 2.135(2) to 2.172(2) Å. The two remaining apical

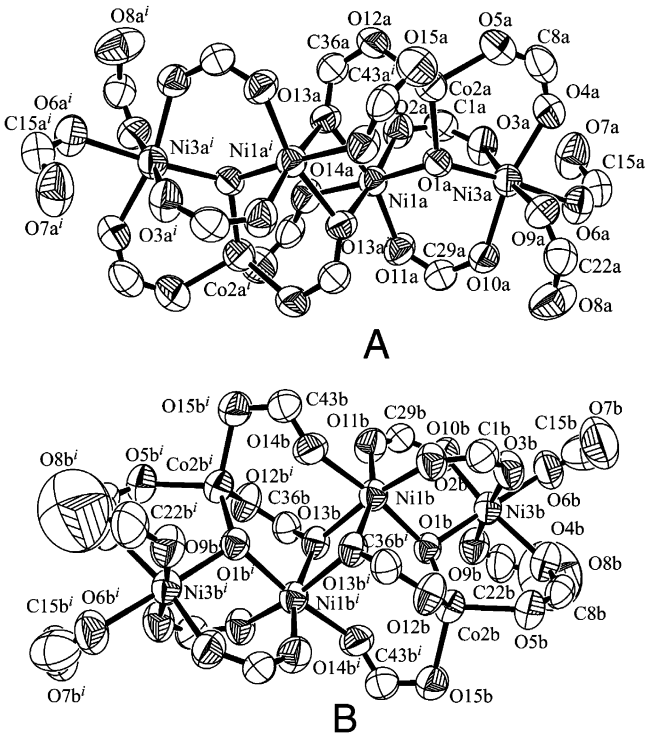

Figure 7. Labeled ORTEP plot at the 50% ellipsoid probability level of the molecules A and B of **VI**. Hydrogen atoms are omitted for clarity.

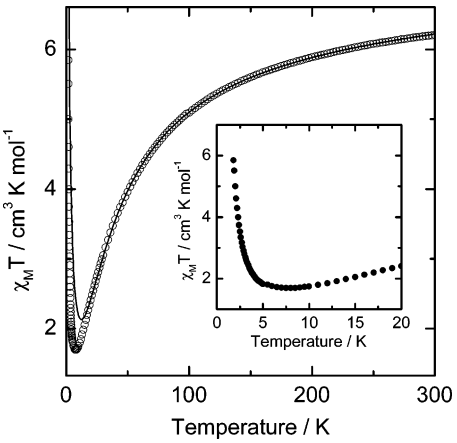

Figure 8. Temperature dependence of $\chi_M T$ product of a powdered sample of **VII**. The circles correspond to the experimental data, and the full line, to the best fitted curve (see text). The inset enhances the minimum of $\chi_M T$ in the low-temperature range.

Table 2. Intramolecular Metal−Metal Distances in Å for **VI**

	molecule A	molecule B
Ni1...Ni3	3.3795(10)	3.4097(10)
Ni1...Co2	3.3378(10)	3.3846(10)
Ni3...Co2	3.4104(11)	3.3872(11)
Ni1...Ni1^a	3.2669(14)	

^{a} 1 − *x*, 1 - *y*, 1 − *z*.

oxygen atoms (Mn3−O10 = 2.187(2) Å and Mn3−O6 = 2.193-(2) Å) behave as η_2 ligands. The O−Mn−O angles between neighboring oxygen atoms range from 86.17(9)° to 95.65(9)°. On both sides, two peripheral nickel ions Ni1 and Ni2 are located in a strongly distorted octahedron [NiO_4N_2]. Two oxygen atoms belonging to the same benzoate anion yield O−Ni−O angles equal to 61.79(8)° and 61.95(8)° for O5−Ni1−O6 and O9−Ni2−O10, respectively; two pyridine ligand are in cis position; the coordination sphere is completed by two oxygen atoms from two different benzoate anions. Intramolecular metal−metal distances are Ni1...Mn3 = 3.5139(5), Ni2...Mn3 = 3.5154(6) Å, and Ni1...Ni2 = 7.0214(5) Å. Two acetonitrile solvent molecules are also present in the asymmetric unit. One of them lies on two positions with occupation factors calculated and fixed to 0.4 and 0.6; the remaining molecule is not disordered. No significant contacts involving non-hydrogen atoms are observed between molecules.

[$Co_2Ni_4(OH)_2(PhCOO)_{10}(PhCOOH)_4$]. The asymmetric unit contains two independent half molecules labeled A and B in Figure 7. The complete molecules are generated by an inversion center. Each molecule contains two cobalt and four nickel ions.

In each asymmetric unit three metal ions share a hydroxide O1 atom. The nickel ions lie in octahedral coordination spheres of six oxygen atoms, and the mean Ni−O bond distance is 2.07 Å for each of the four octahedra. Molecule B possesses less regular octahedra than A. Five oxygen atoms of the [$Ni1O_6$] coordination environment belong only to four different benzoate ions. Three of them (O2, O11, O14) come from $\mu_2(\eta_1,\eta_1)$ benzoate bridges, whereas the remaining O13 and its symmetrical equivalent are in η_2 modes and come from the $\mu_3(\eta_1,\eta_2)$ benzoate. The longest Ni1−O bond distance is Ni1A−O13A = 2.169(4) Å [Ni1B−O13B = 2.162(3) Å] whereas the shortest is Ni1A−O2A = 2.003(4) Å) [Ni1B−O10B = 1.992(4) Å)]. The sixth coordination position is occupied by the O1 oxygen from the μ_3-OH^- bridge. Five oxygens in the $Ni3O_6$ octahedron belong to three μ_2 bridging benzoates ions (O3, O4, O10) and two molecules of benzoic acid (O6, O9). The longest Ni3−O bond distances are Ni3A−O9A = 2.116(4) Å [Ni3B−O6B = 2.141(5) Å] whereas the shortest are Ni3A−O4A = 2.025(4) Å [Ni3B−O10B = 2.004(4) Å], and the O−Ni3−O angles between neighboring oxygen atoms are ranging from 82.68-(16)° to 98.84(16)° [82.34(19)° to 100.28(19)° in molecule B]. The cobalt ions lie in a tetrahedral coordination sphere where three oxygen atoms (O5, O12, O15) belong to three $\mu_2(\eta_1,\eta_1)$ benzoate ligands. The inversion center close to Ni1 ions yields the entire molecule, as [$Ni1O_6$] octahedra are sharing their O13−O13 edge. The shortest intramolecular metal−metal distances are given in Table 2. No significant contacts involving non-hydrogen atoms are observed between molecules.

Magnetic Properties. The temperature dependence of $\chi_M T$ of **VII** (χ_M is molar magnetic susceptibility, and *T*, the temperature in Kelvin) is displayed in Figure 8. The magnetic behavior is typical of ferrimagnetic chains.[14] The room temperature $\chi_M T$ value is equal to 6.85 cm^3 K mol^{-1}. On lowering the temperature, $\chi_M T$ decreases, passes through a broad minimum at 7 K, and then increases. The decrease of $\chi_M T$ is due to antiferromagnetic interactions between cobalt and manganese spins, whereas the increase at low temperature is due to an effective ferromagnetic interaction between antiferromagnetically coupled MnCo pairs. The high-temperature range ($T >$ 100 K) can be fitted with Curie−Weiss law ($\chi_M = C/(T - \theta)$). We find C = 6.97 cm^3 K mol^{-1} and $\theta = -37$ K. It is well-known that the Zeeman factor for octahedral Mn(II) is close to 2.00. Keeping this in mind along with $S_{Mn} = {}^5/_2$ and $S_{Co} = {}^3/_2$ we find an average g_{Co} value equal to 2.35 in agreement with

(14) Kahn, O. *Molecular Magnetism*; VCH: New York, 1993.

other tetrahedral Co(II) complexes.[15,16] Better estimation of the strength of the superexchange interaction between Mn(II) and Co(II) can be obtained by fitting the data above 30 K, considering that both S_{Mn} and S_{Co} are classical spins.[17] With the Hamiltonian

$$H = \sum_{i=1}^{n}(-J\boldsymbol{S}_{Mn_i}\cdot\boldsymbol{S}_{Co_i} - J\boldsymbol{S}_{Co_i}\cdot\boldsymbol{S}_{Mn_i+1} + (g_{Mn}\boldsymbol{S}_{Mn_i} + g_{Co}\boldsymbol{S}_{Co_i})\cdot\boldsymbol{H})$$

$\chi_M T$ is expressed as follow:

$$\chi_M T = \frac{2N\beta^2}{3k}\left[g^2\frac{1+u}{1-u} + \delta^2\frac{1-u}{1+u}\right]$$

with

$$g = \frac{1}{2}(g^e_{Mn} + g^e_{Co}) \text{ and } \delta = \frac{1}{2}(g^e_{Mn} - g^e_{Co})$$

$$g^e_{Mn} = g_{Mn}\sqrt{S_{Mn}(S_{Mn}+1)},\ g^e_{Co} = g_{Co}\sqrt{S_{Co}(S_{Co}+1)}$$

$$J^e = J\sqrt{S_{Mn}(S_{Mn}+1)}\sqrt{S_{Co}(S_{Co}+1)},\ u = \coth\left(\frac{J^e}{kT}\right) - \frac{kT}{J^e}$$

The other parameters have their usual meanings. The best fit with $S_{Mn} = {}^5/_2$ and $S_{Co} = {}^3/_2$ in the temperature range 30−300 K is obtained with $g_{Mn} = 2.024 \pm 0.002$, $g_{Co} = 2.199 \pm 0.003$, and $J = -5.576 \pm 0.020$ cm^{-1} (see Figure 8). The agreement between the experiment and the theory is fairly good even if the model is oversimplified with g_{Co} in the range of commonly admitted values for Co(II) in a tetrahedral environment. It would not be reasonable to fit the data down to 4 K (to reproduce the minimum in $\chi_M T$) for three reasons; (i) In a tetrahedral environment the $^4A_2$ ground state manifold of Co(II) is split by Zero Field Splitting (ZFS) which is usually found on the order of ± 10 cm^{-1}.[18] This magnetic anisotropy affects the low temperature data. Also, slightly anisotropic g values are commonly encountered;[18] (ii) Two adjacent Mn(II) ions in a chain are bounded by $\mu_3(\eta_1,\eta_2)$ benzoate bridges and may therefore interact. To confirm or infirm this hypothesis we synthesized a MnZn chain where the diamagnetic Zn(II) occupies tetrahedral sites. The χ_M vs T curve (not represented) of a powdered sample of MnZn passes through a broad maximum at $T_{max} = 4$ K. This clearly indicates that antiferromagnetic interactions between Mn centers operate. The experimental data can be fitted with a theoretical expression derived by Fischer using the classical spin approximation.[19] The superexchange parameter between two Mn(II) neighbors is found at -0.619 ± 0.002 cm^{-1}; (iii) the classical spin approximation is certainly not valid down to the lowest temperature.

The magnetic anisotropy in **VII** is evidenced by single-crystal measurements. On Figure 9 are represented the temperature dependences of the $\chi_M T$ products with the magnetization recorded on single crystals with the external field parallel ($\chi_M T_{||}$) and perpendicular ($\chi_M T_\perp$) to the chain axis (a axis). Above 15 K both curves are nearly parallel but do not coincide with $\chi_M T_\perp > \chi_M T_{||}$. This difference is due to the Zeeman anisotropy. Below 15 K thermal behaviors differ dramatically. On one hand, $\chi_M T_{||}$ passes through a minimum at $T = 11$ K and increases very rapidly on cooling to 2 K. On the other hand, the minimum in $\chi_M T_\perp$ is located at $T = 4$ K with a small increase down to 2 K.[20] At 2 K, $\chi_M T_{||}$ is more than fifteen times bigger than $\chi_M T_\perp$. These measurements reveal uniaxial symmetry with the easy magnetization axis parallel to the chain axis. The anisotropy is confirmed by the field dependence of the magnetization at low temperature (see Figure 10). Indeed, at $T = 2$ K, it increases very rapidly in a low field when the external magnetic field is applied along the a axis, and then the magnetization increases linearly and smoothly above 1 T and up to 5 T. No magnetic hysteresis loop can be detected. The magnetization in the perpendicular direction increases more slowly in all the field range and also without hysteresis. Surprisingly the two curves cross at 3 T. This could reflect a subtle balance between single-ion ZFS, the anisotropy of the g-factors, and the Zeeman energy. One must keep in mind that the rapid increase of the magnetization parallel to the chain does not imply three-dimensional

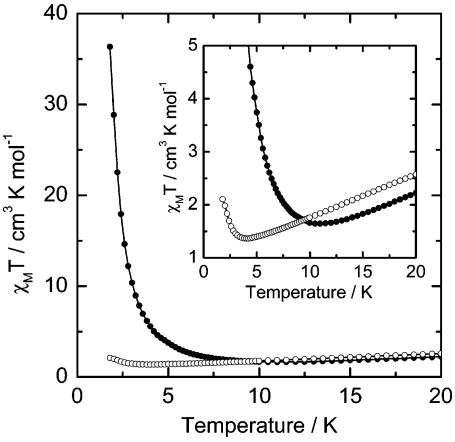

Figure 9. Temperature dependence of $\chi_M T$ product of **VII** with the magnetic field applied parallel (black dots) and perpendicular (white dots) to the chain axis. The inset is a zoom on the minima. The full lines are eye guides only.

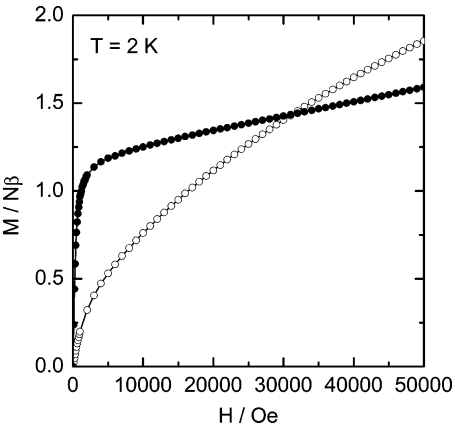

Figure 10. Field dependences of the magnetization measured at $T = 2$ K on single crystals of **VII** with the magnetic field parallel (black dots) and perpendicular (white dots) to the chain axis. The full lines are eye guides only.

(15) Carlin, R. L. *Magneto-chemistry*; Springer-Verlag: New York, 1986.
(16) Abragam, A.; Bleaney, B. *Electron paramagnetic Resonance of Transition Ions*; Dover Publications: New York, 1970.
(17) Drillon, M.; Coronado, E.; Beltran, D.; Georges, R. *Chem. Phys.* **1983**, *79*, 449.
(18) Krzystek, J.; Zvyagin, S. A.; Ozarowski, A.; Fiedler, A. T.; Brunold, T. C.; Telser, J. *J. Am. Chem. Soc.* **2004**, *126*, 2148. Nelson, D.; ter Haar, L. W. *Inorg. Chem.* **1993**, *32*, 182.
(19) Fisher, M. E. *Am. J. Phys.* **1964**, *32*, 343.
(20) The increase below 4 K may be real or the consequence of misorientation of crystals.

magnetic order because it is compatible with one-dimensional correlations in Ising systems. The field dependences of Single Chain Magnets (SCM),[21a−h] which are also Ising chains, behave the same.[21b] To clearly establish the low-temperature magnetic state, a.c. susceptibility measurements are required. Indeed, SCM shows slow relaxation of the magnetization with relaxation time characteristic of a thermally activated process; the a.c. susceptibility is therefore frequency dependent. One must not exclude that short interchain contacts may take place at low temperature and establish three-dimensional magnetic order.

Conclusion

A convenient one-pot route for the synthesis of transition metal polynuclear complexes is accomplished. It is based on the in situ generation of carbolxylate ligands by oxidation of aromatic aldehydes by metal nitrates in air, followed by isolation of target compounds by specific solvent choices. This method bypasses the direct use of transition metal carboxylate salts as starting materials. Indeed, they are not soluble in noncoordinating solvents which strongly limits the flexibility of the synthesis processes. Another remarkable feature of this method is its successful extension to the synthesis of heterometallic polynuclear complexes using stoichiometric amounts of starting metal ions. Several series of discrete tri-, tetra-, hexa, and octanuclear as well as 1D chain compounds were hence obtained with appreciable yields and significant short reaction times. Our finding is illustrated in this paper by benzaldehyde and either Co nitrate in the case of homometallic complexes or Co, Ni, and Mn nitrates for heterometallic compounds. This opens a wide possibility for molecular construction of transition metal complexes with different nuclearity tunings by simple solvent variation at the second step.

Acknowledgment. Financial support from CNRS, INTAS Grant 03-51-4532. K.S.G. is grateful to NATO for his postdoctoral fellowship.

Supporting Information Available: X-ray crystallographic file (CIF). This material is available free of charge via the Internet at http://pubs.acs.org.

JA050451P

(21) (a) Caneschi, A.; Gatteschi, D.; Lalioti, N.; Sangregorio, C.; Sessoli, R.; Venturi, G.; Vindigni, A.; Rettori, A.; Pini, M. G.; Novak, M. A. *Angew. Chem., Int. Ed.* **2001**, *40*, 1760. (b) Clérac, R.; Miyasaka, M.; Yamashita, M.; Coulon, C. *J. Am. Chem. Soc.* **2002**, *124*, 12837. (c) Liu, T. F.; Fu, D.; Zhang, Y.-Z.; Sun, H.-L.; Su, G.; Liu, Y.-J. *J. Am. Chem. Soc.* **2003**, *125*, 13976. (d) Miyasaka, H.; Clérac, R.; Mizushima, K.; Sugiura, K.-I.; Yamashita, M.; Wernsdorfer, W.; Coulon, C. *Inorg. Chem.* **2003**, *42*, 8203. (e) Pardo, E.; Ruiz-Garcia, R.; Lloret, F.; Faus, J.; Julve, M.; Journaux, Y.; Delgado, F.; Ruiz-Pérez, C. *Adv. Mater.* **2004**, *16*, 1597. (f) Costes, J.-P.; Clemente-Juan, J. M.; Dahan, F.; Milon, J. *Inorg. Chem.* **2004**, *43*, 8200. (g) Wang, S.; Zuo, J.-L.; Gao, S.; Song, Y.; Zhou, H.-C.; Zhang, Y.-Z.; You, X.-Z. *J. Am. Chem. Soc.* **2004**, *126*, 8900. (h) Lescouëzec, R.; Vaissermann, J.; Ruiz-Pérez, C.; Lloret, F.; Carrasco, R.; Julve, M.; Verdaguer, M.; Dromzee, Y.; Gatteschi, D.; Wernsdorfer, W. *Angew. Chem., Int. Ed.* **2003**, *42*, 1483.